
Latent Thought Flow: Efficient Latent Reasoning in Large Language Models

Xiandong Zou¹, Jing Huang², Jianshu Li², Pan Zhou^{1*}
¹Singapore Management University ²Ant Group

Abstract

Large Language Models (LLMs) increasingly rely on intermediate reasoning, yet explicit Chain-of-Thought (CoT) suffers from a linguistic space bottleneck: each thought must be decoded into tokens, causing high inference overhead. Latent reasoning moves deliberation into continuous space, but existing methods mostly learn deterministic or reward-maximizing paths, lacking a principled way to allocate probability across trajectories with different correctness and costs. We propose **Latent Thought Flow (LTF)**, which models reasoning as variable-length continuous trajectories and trains a sampler to match a reward-induced posterior over answer quality and computation cost. We instantiate this with a continuous GFlowNet using stochastic latent transitions. To handle sparse answer supervision, we introduce an Entropy-Weighted Subtrajectory Balance objective for intermediate rewards and a reference-prior regularizer to anchor exploration. Experiments under finetuning and transfer learning settings show that LTF outperforms explicit CoT and latent reasoning baselines, improving accuracy by 9.5% while reducing reasoning length by 27.2% on average compared with strong latent reasoning baselines.

1 Introduction

Large Language Models (LLMs) [1–4] are increasingly tasked with complex objectives that demand a synergy of perception and deliberation, ranging from math problem solving [5, 6], embodied planning [7, 8], and code generation [9, 10]. A cornerstone of this success is the use of intermediate reasoning processes, where frameworks like Chain-of-Thought (CoT) [11, 12], Self-Consistency [13], and Tree-of-Thoughts [14] decompose intricate problems into sequential rationales. While promising, they inevitably encounter a *linguistic space bottleneck*: the requirement to decode every intermediate thought into discrete tokens. The explicit reasoning not only incurs substantial inference overhead but also constrains the model’s internal computation into a potentially redundant textual form. Consequently, this reliance on explicit rationales creates an inherent accuracy–efficiency trade-off, limiting the scalability of reasoning capabilities in resource-constrained scenarios.

Latent reasoning has emerged as a promising alternative to mitigate the linguistic space bottleneck by performing multi-step computation directly within the model’s continuous hidden-state space. Rather than fully externalizing deliberation as discrete text, these approaches keep intermediate reasoning internalized: Pause tokens [15] allocate additional latent computation; stepwise internalization and compressed CoT [16, 17] densify textual rationales; and other frameworks [18–24] like Coconut propagate continuous thought vectors or soft representations via the LLM backbone. These works demonstrate that meaningful intermediate computation need not always be expressed in linguistic words. However, most existing approaches primarily define a deterministic latent reasoning path and train it by compression, distillation, or reward maximization under a fixed reasoning budget. They do not specify how sampling probability mass should be allocated across latent reasoning trajectories with different correctness and computational costs under various questions.

*Corresponding author.

We argue that this missing distributional view is central to efficient latent reasoning. For a given question, an LLM must navigate a manifold of plausible reasoning paths and only a sparse subset of which yields both logical consistency and computational efficiency. Without this distributional perspective, existing paradigms often fail to optimize the latent reasoning manifold: maximum-likelihood objectives inherit the verbosity of training rationales, while reinforcement learning tends to trigger posterior collapse onto a few high-reward modes. What is required is *a principled sampler capable of modeling the trade-offs between correctness and computational cost*. Such a framework should concentrate probability mass on concise and accurate trajectories while suppressing redundant or erroneous paths, thereby enabling the model to dynamically allocate its computational budget.

In this paper, we propose **Latent Thought Flow (LTF)**, a reward-proportional framework for learning continuous latent reasoning in LLMs. Given a question x , LTF samples a latent reasoning trajectory $\tau = (\mathbf{z}_{1:T}, \perp)$, where each \mathbf{z}_t is a continuous thought state in LLM’s latent space and \perp denotes an adaptive stopping decision. The LLM then produces the final response conditioned on x and τ (Fig. 1). During training, the target answer defines a utility $\mathcal{R}_{x,y}(\tau)$ consisting of answer quality and computation cost, inducing the desired posterior over latent thoughts,

$$p^*(\tau | x, y) \propto \mathcal{R}_{x,y}(\tau). \quad (1)$$

We train the latent sampler to match this reward-induced distribution with a continuous GFlowNet objective. GFlowNets are designed to learn stochastic generative policies whose terminal samples are proportional to an unnormalized reward, which makes them well suited for preserving diverse high-utility solutions rather than only optimizing for a single maximum-reward trajectory [25, 26]. While recent work has applied GFlowNets to LLM or VLM reasoning over discrete texts, proof, or action traces [27–29], LTF moves reward-proportional trajectory learning into LLM’s latent space.

This formulation introduces three technical challenges. First, latent thoughts are high-dimensional continuous vectors, so discrete token-level balance equations are not directly applicable. Building on continuous GFlowNet theory [30], LTF parameterizes forward transitions with conditional densities and writes balance constraints over variable-length continuous trajectories. Second, answer-level supervision is sparse: the utility of a latent subtrajectory is typically observed only after the final response. We therefore use a Subtrajectory Balance objective [31, 32] with entropy-aware weighting to propagate terminal rewards to intermediate latent subtrajectories. Third, unconstrained exploration in a continuous latent space can drift away from meaningful latent states. LTF addresses this with a reference-prior regularizer that warm-starts exploration from modality-aligned anchors, while annealing the prior so that learned trajectories are shaped by the accuracy–efficiency reward. During inference, LLM samples latent thought paths and generates answers without access to gold rationales.

Experiments demonstrate that LTF improves the accuracy–efficiency frontier of reasoning, reduces reasoning overhead, and adapts its latent budget to problem difficulty compared with explicit CoT, latent reasoning, and reward-maximizing baselines. Compared with strong latent reasoning baselines CoLaR and ReGuLaR, LTF improves accuracy by 12.9% while reducing reasoning length by 34.5% on average in fine-tuning tasks; under transfer learning, LTF improves accuracy by 6.0% while reducing reasoning length by 19.9% on average.

2 Related Work

Explicit Chain of Thought (CoT). A common approach to reasoning exposes intermediate computation as text. CoT prompting elicits rationales [11, 12], self-consistency aggregates sampled rationales [13], and Tree-of-Thoughts searches textual states [14]. Multimodal variants produce explanations or grounded rationales, e.g., ScienceQA [33], Multimodal-CoT [34], and Visual CoT [35], while tool- and program-based systems externalize reasoning via vision experts or executable programs [36, 37]. Although interpretable, these methods serialize visual, spatial, and perceptual computation into lengthy language, programs, or actions. LTF instead uses latent trajectories, reducing decoding overhead while retaining adaptive computation before final answer generation.

Latent Reasoning. To reduce the cost of long textual rationales, recent work explores reasoning in LLM latent spaces. Pause tokens add hidden computation before decoding [15]; explicit-to-implicit training gradually removes CoT supervision [16]; and continuous-thought methods replace rationales with dense contemplation tokens, recurrent states, or soft thought tokens [17–21, 38]. Other methods learn abstract discrete tokens [39] or probabilistic latent vectors with posterior inference [22, 40–42].

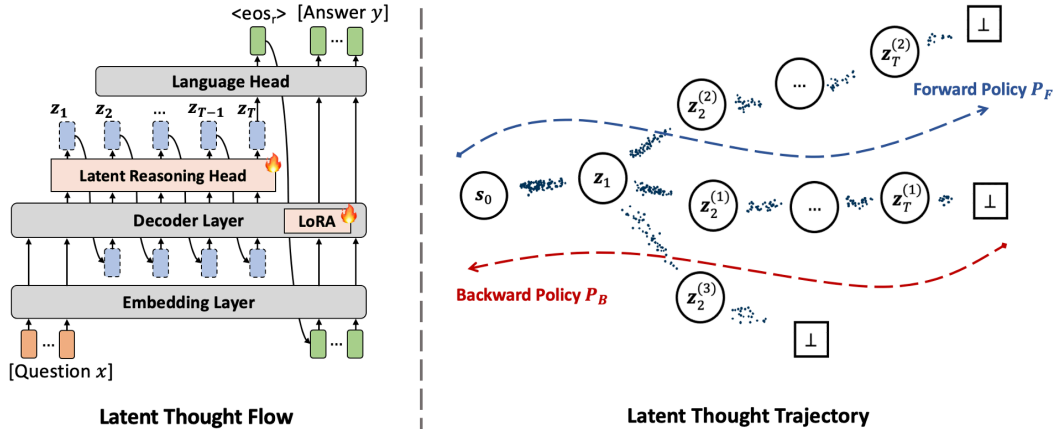


Figure 1: Illustration of our **LTF** framework. *Left*: Overall architecture of **LTF**. Only the LoRA module and latent reasoning head are trainable. *Right*: Overview of latent thought trajectories from a continuous GFlowNet perspective. A latent reasoning trajectory is represented as $\tau = (s_0, z_1, \dots, z_T, \perp)$, where z_t denotes the latent thought state at step t . The forward policy P_F is parameterized as a variational sampling via LLM with a latent head (Eq. (3)) and trained with our entropy-weighted subtrajectory balance objective (Eq. (18)) to achieve the flow balance condition.

Unlike methods that imitate or compress a single reasoning trace, LTF learns a reward-induced posterior over variable-length latent reasoning trajectories.

GFlowNets for Diverse Reasoning. Generative Flow Networks learn a policy whose terminal distribution is proportional to an unnormalized reward [25, 26], providing a distribution-matching alternative to reinforcement-learning-based latent reasoning that typically maximizes expected reward [23, 24, 43, 44]. By preserving probability mass over multiple high-reward solutions, GFlowNets naturally support diverse reasoning. Trajectory Balance [31] and continuous-space GFlowNets [30] further enable textual reasoning [45, 46] and visual rationale generation [27, 29, 47]. However, existing GFlowNet-based methods mainly model explicit textual, symbolic, or visual traces, with limited focus on reasoning efficiency. In contrast, LTF samples in continuous latent superposition space, enabling adaptive computation and favoring trajectories that are both accurate and efficient.

3 Methodology

Overview. Latent Thought Flow (LTF) models reasoning as an adaptive flow over continuous latent thought states before generating the final answer (Fig. 1). Rather than committing to a single deterministic latent thought chain or relying on explicit textual rationales, LTF learns a distribution over variable-length latent reasoning trajectories. Its guiding principle is that *a trajectory should be sampled with high probability when it solves the problem accurately using minimal computation, and with low probability when it is incorrect or redundant*. We instantiate this principle with a continuous GFlowNet objective, which trains a reward-proportional sampler over latent trajectories [25, 26, 30]. Concretely, LTF consists of four components: a variable-length latent thought sampler (Sec. 3.1), an accuracy–efficiency reward (Sec. 3.2), a continuous Subtrajectory Balance objective (Sec. 3.3), and a reference-prior regularizer (Sec. 3.4) that keeps early exploration semantically grounded.

3.1 Variable-Length Latent Thought Trajectories

LTF replaces explicit textual rationales with an adaptive latent reasoning process: instead of forcing the model to learn deterministic reasoning tokens, it learns “how much” to reason internally before producing the final answer. Given a training set $\mathcal{D} = \{(x, y, r)\}$, where x can be an input containing a question or instruction, y is the target answer, and r is an optional reference rationale used only for training, we would like to train an LLM p_Θ with the latent reasoning mechanism. Let $\Theta = \{\phi, \psi\}$ denote the model parameters, where p_ϕ consists of the embedding and decoder layers that produce contextual latent states, and p_ψ denotes the language head that generates explicit tokens (Fig. 1).

Formally, given an input x , LTF samples a variable-length latent thought trajectory

$$\tau = (\mathbf{z}_{1:T}, \perp) \in \mathcal{T}, \quad \mathbf{z}_t \in \mathbb{R}^{d_z}, \quad 0 \leq T \leq T_{\max}, \quad (2)$$

where T denotes the number of continuous latent thoughts and \perp denotes termination ($T = 0$ means answering without reasoning). Let $h_x = p_\phi(x)$ and $s_t = (h_x, \mathbf{z}_{1:t})$. To build a variational latent reasoning process with expressive latent superposition states, each latent thought \mathbf{z}_t is sampled by a sampler q_ϕ consisting of a decoder layer and a latent reasoning head (Fig. 1).

At each step t , conditioned on the current context s_t , with $s_0 = h_x$, the LLM samples each latent reasoning state from its posterior distribution given the question and the previous ones, i.e., $z_t \sim q_\phi(\cdot | s_t)$. In this study, we model the latent policy q_ϕ as the Gaussian distribution following prior work [41, 42], and it samples the latent thoughts from a continuous density iteratively until achieving the decoded $\langle \text{eos}_r \rangle$ token:

$$q_\phi(\mathbf{z}_{t+1} | s_t) = \mathcal{N}(\boldsymbol{\mu}_\phi(s_t), \text{diag}(\boldsymbol{\sigma}_\phi^2(s_t))), \quad \pi^\perp(s_t) = p_\psi(\langle \text{eos}_r \rangle | s_t), \quad (3)$$

with the reparameterization $\mathbf{z}_{t+1} = \boldsymbol{\mu}_\phi(s_t) + \boldsymbol{\sigma}_\phi(s_t) \odot \boldsymbol{\epsilon}$, $\boldsymbol{\epsilon} \sim \mathcal{N}(0, I)$, which allows gradients from the answer loss to pass through the latent computation [48]. The resulting trajectory density is

$$q_\phi(\tau | x) = \left[\prod_{t=0}^{T-1} (1 - \pi^\perp(s_t)) q_\phi(\mathbf{z}_{t+1} | s_t) \right] \pi^\perp(s_T), \quad \tau = (\mathbf{z}_{1:T}, \perp). \quad (4)$$

where the product is empty when $T = 0$. We force $\pi^\perp(s_{T_{\max}}) = 1$ when the maximum budget T_{\max} is reached. Eq. (4) provides the prerequisite for an adaptive reasoning budget by modeling a distribution over variable-length latent trajectories. This allows LTF, in principle, to assign shorter trajectories to easier examples and longer trajectories to harder ones.

Given the prefix and latent thought tokens, the answer can be generated:

$$p_\psi(y | x, \tau) = \prod_{m=1}^{|y|} p_\psi(y_m | \tau, y_{<m}). \quad (5)$$

Learning such latent reasoning trajectories is challenging for three reasons. First, reasoning states are unobserved, continuous, and variable-length, with no token-level supervision for identifying informative intermediate computations. The model must infer both what to compute and when to stop from the final answer quality alone. Second, many trajectories may yield the same correct answer, but differ in computational efficiency, so optimizing a single best path is insufficient; probability should reflect both accuracy and cost. Third, latent thought spans a high-dimensional continuous space, where naive exploration is unstable and prone to semantically meaningless states.

3.2 Reward-Proportional Target Distribution

Since latent thoughts are unobserved, LTF specifies their desired behavior through a terminal reward rather than step-level supervision. For each training pair (x, y) , we assign a trajectory $\tau = (s_T \rightarrow \perp)$ a non-negative accuracy–efficiency utility

$$\mathcal{R}_{x,y}(\tau) = V_{x,y}(\tau) \exp(-\lambda_c C(\tau)), \quad (6)$$

where $V_{x,y}(\tau)$ measures answer quality, $C(\tau)$ measures latent computation, λ_c controls the cost penalty. We instantiate the quality score as

$$V_{x,y}(\tau) = \text{Ver}(y, \hat{y}_\tau) + \exp(1/|y| \cdot \log p_\psi(y | x, \tau)), \quad (7)$$

where \hat{y}_τ is the decoded answer and Ver denotes the task-specific accuracy. The verifier term aligns the reward with the evaluation metric, while the normalized likelihood term provides a dense signal. By default, we use a length-based cost function

$$C(\tau) = T, \quad (8)$$

which favors shorter latent trajectories unless additional computation improves answer quality.

This reward induces the target distribution over terminal latent trajectories:

$$p^*(\tau | x, y) = \mathcal{R}_{x,y}(\tau) / Z_{\mathcal{R}}(x, y), \quad Z_{\mathcal{R}}(x, y) = \int_{\mathcal{T}} \mathcal{R}_{x,y}(\tau) d\tau. \quad (9)$$

LTF learns not a single optimal path, but a reward-proportional distribution where multiple correct and efficient trajectories coexist, while incorrect or inefficient ones receive low mass. Because $Z_{\mathcal{R}}(x, y)$ integrates over continuous latent trajectories of all lengths, direct normalization is intractable. We thus train the amortized sampler $q_\phi(\tau | x)$ to match this target. The answer y defines rewards only during training; at inference, the sampler conditions solely on x .

3.3 Continuous GFlowNet

GFlowNets train a stochastic generator to sample complete trajectories in proportion to a positive reward, rather than only maximizing the expected reward of a single trajectory [25, 26]. This property is well suited for latent reasoning, where multiple internal thought paths may lead to the same correct answer and should therefore be preserved during training. In LTF, the latent thoughts are continuous density, so the discrete transition probability in standard GFlowNets becomes a continuous transition density. To provide dense supervision for intermediate latent prefixes, we allow every prefix state to terminate: after stopping at a prefix, the model decodes an answer and receives a reward. This allows us to compute the flow of each prefix analytically from its immediate-stop reward and stop probability, avoiding an additional learned flow estimator.

For a subtrajectory $s_i \rightarrow s_{i+1} \rightarrow \dots \rightarrow s_j$, the GFlowNet flow balance condition requires

$$F(s_i) \prod_{t=i}^{j-1} P_F(s_{t+1} | s_t) = F(s_j) \prod_{t=i}^{j-1} P_B(s_t | s_{t+1}), \quad (10)$$

where $F(s_i)$ is the flow at state s_i , and P_F and P_B denote the forward and backward transitions, respectively. Since our state $s_t = (h_x, \mathbf{z}_{1:t})$ stores the full latent prefix, each state has a unique parent obtained by removing the last latent vector. Thus, the backward transition is deterministic and contributes zero log-density along a valid trajectory.

Under our latent thought trajectory formulation in Sec. 3.1, the forward transition density from s_t to non-terminal state s_{t+1} is given by

$$P_F(s_{t+1} | s_t) = (1 - \pi^\perp(s_t)) q_\varphi(\mathbf{z}_{t+1} | s_t), \quad (11)$$

where $q_\varphi(\mathbf{z}_{t+1} | s_t)$ is the Gaussian density defined in Eq. (4), and $\pi^\perp(s_t)$ is the probability of stopping at s_t . Therefore, the forward edge log-density for a non-terminal transition is

$$\ell_t^\varphi = \log q_\varphi(\mathbf{z}_{t+1} | s_t) + \log(1 - \pi^\perp(s_t)). \quad (12)$$

Since the reward $\mathcal{R}_{x,y}(s_t \rightarrow \perp)$ of terminating at prefix s_t is defined in Eq. (6), where the model stops at s_t , decodes an answer, and scores it against the training answer y , the flow $F(s_t)$ can be expressed by the terminal consistency condition

$$F(s_t) \pi^\perp(s_t) = \mathcal{R}_{x,y}(s_t \rightarrow \perp) \Rightarrow F(s_t) = \frac{\mathcal{R}_{x,y}(s_t \rightarrow \perp)}{\pi^\perp(s_t)}. \quad (13)$$

Thus, the flow of an intermediate prefix does not need to be learned by a separate network; it can be computed from the reward obtained by immediately stopping at that prefix.

We use Sub-Trajectory Balance [32] objective to enforce this consistency over all subtrajectories due to its stable optimization and low variance property [26, 49]. For $0 \leq i < j \leq T$, the residual is

$$\begin{aligned} \chi_{i:j} &= \log F(s_i) + \sum_{t=i}^{j-1} \ell_t^\varphi - \log F(s_j) \\ &= \log \frac{\mathcal{R}_{x,y}(s_i \rightarrow \perp) \left[\prod_{t=i}^{j-1} q_\varphi(\mathbf{z}_{t+1} | s_t) (1 - \pi^\perp(s_t)) \right] \pi^\perp(s_j)}{\mathcal{R}_{x,y}(s_j \rightarrow \perp) \pi^\perp(s_i)}. \end{aligned} \quad (14)$$

Thus, the continuous Sub-Trajectory Balance objective is

$$\mathcal{L}_{\text{SubTB}}(x, y) = \mathbb{E}_{\tau \sim q_\varphi(\cdot | s_0)} \left[\sum_{0 \leq i < j \leq T} \chi_{i:j}^2 \right]. \quad (15)$$

Minimizing this loss encourages the latent sampler to assign larger density to reasoning trajectories whose prefixes and completions obtain higher answer rewards, while preserving multiple valid reasoning paths instead of collapsing to a single mode.

Entropy-Weighted Subtrajectory Balance. Treating all subtrajectories uniformly is suboptimal: low-entropy paths are locally concentrated, while high-entropy paths usually correspond to regions with richer spread of information where the sampler needs stronger supervision [43, 46, 49]. We therefore introduce *Entropy-Weighted Subtrajectory Balance* (EW-SubTB), which uses the relative entropy of latent subtrajectories to reweight residuals without changing the reward-proportional objective. This entropy-aware weighting enables effective allocation of supervision across subtrajectories.

Given S sampled trajectories for the same input x , we define the entropy for the latent $\mathbf{z}_{t+1}^{(s)}$ as $h_t^{(s)} = \mathcal{H}[q_\varphi(\mathbf{z}_{t+1}^{(s)} | s_t^{(s)})]$ where $\mathcal{H}(\cdot)$ denotes differential entropy. For a subtrajectory $s_i \rightarrow \dots \rightarrow s_j$, the length-normalized entropy is given by $\bar{h}_{i:j}^{(s)} = \frac{1}{j-i} \sum_{t=i}^{j-1} h_t^{(s)}$. Thus, the entropy-aware weight is

$$\omega_{i:j}^{(s)} = \text{sg} \left[\exp(\bar{h}_{i:j}^{(s)}) / (1/|\mathcal{S}_{i:j}| \cdot \sum_{r \in \mathcal{S}_{i:j}} \exp(\bar{h}_{i:j}^{(r)})) \right], \quad (16)$$

where $\mathcal{S}_{i:j}$ denotes the set of subtrajectories between indices i and j in S sampled trajectories, and $\text{sg}[\cdot]$ denotes the gradient stopping operation. This weighting keeps the average scale of the loss stable while assigning larger weights to relatively high-entropy latent reasoning subtrajectories.

For each sampled trajectory, the continuous SubTB residual is

$$\chi_{i:j}^{(s)} = \log \frac{\mathcal{R}_{x,y}(s_i^{(s)} \rightarrow \perp) \left[\prod_{t=i}^{j-1} q_\varphi(\mathbf{z}_{t+1}^{(s)} | s_t^{(s)}) (1 - \pi^\perp(s_t^{(s)})) \right] \pi^\perp(s_j^{(s)})}{\mathcal{R}_{x,y}(s_j^{(s)} \rightarrow \perp) \pi^\perp(s_i^{(s)})}. \quad (17)$$

The empirical EW-SubTB objective is

$$\mathcal{L}_{\text{flow}}(x, y) = \frac{1}{S} \sum_{s=1}^S \sum_{0 \leq i < j \leq T^{(s)}} \omega_{i:j}^{(s)} \left(\chi_{i:j}^{(s)} \right)^2. \quad (18)$$

Since $\omega_{i:j}^{(s)}$ only reweights the squared residual and is not inserted into the balance ratio, EW-SubTB changes the optimization emphasis but preserves the same reward-proportional target distribution. Our proposed objective is validated via both empirical results (Sec. 4) and analysis (Appendix C.2).

3.4 Reference-Prior Regularization

Reward-proportional learning is difficult at the beginning of training because randomly explored continuous thoughts may not correspond to meaningful latent thoughts in the latent space. To ground early exploration, LTF uses a reference prior derived from teacher-generated reasoning traces when they are available [34, 35]. The prior anchors latent thoughts to meaningful regions of latent space, and the GFlowNet reward later reshapes the sampler toward concise and correct trajectories.

Given a reference latent rationale r for input x , we introduce a reference branch after the decoder layer similar to the latent reasoning head. We define the reference transition density $p_{\theta'}^{\text{ref}}$ as:

$$p_{\theta'}^{\text{ref}}(\mathbf{z}_t | s_{t-1}) = \mathcal{N}(\mathbf{z}_t; \boldsymbol{\mu}_{\theta'}(s_{t-1}), \text{diag}(\boldsymbol{\sigma}_{\theta'}^2(s_{t-1}))). \quad (19)$$

The reference branch anchors the latent space semantically to optimize the LoRA attached to the backbone encoder layer. We regularize the prior sampler by aligning it to the reference prior:

$$\mathcal{L}_{\text{prior}} = -\mathbb{E}_{(x,r) \sim \mathcal{D}} [\log p_{\theta'}^{\text{ref}}(r | x)]. \quad (20)$$

Thus, early training benefits from semantically grounded latent states with stable exploration, while later training is governed by the accuracy–efficiency reward. If no rationale is available, this term is omitted and LTF trains only from answer supervision and the reward.

3.5 Training Objective and Inference

The training objective consists of complementary components for latent-thought sampling and answer prediction. The flow loss trains the sampler to allocate probability mass according to reward, while the cross entropy loss ensures that sampled thoughts remain effective for deriving the correct answer. Given an input-answer pair (x, y) , we define the answer loss as

$$\mathcal{L}_{\text{ans}}(x, y) = -\mathbb{E}_{\tau \sim q_\varphi(\cdot | H_x)} [\log p_\psi(y | \tau)]. \quad (21)$$

When computing the flow loss, we stop gradients through the scalar reward $\mathcal{R}_{x,y}(\tau)$; this prevents the decoder from changing the reward scale to satisfy balance and leaves answer learning to Eq. (21). The final objective is

$$\mathcal{L} = \mathcal{L}_{\text{flow}} + \lambda_{\text{ans}} \mathcal{L}_{\text{ans}} + \lambda_{\text{prior}} \mathcal{L}_{\text{prior}}, \quad (22)$$

where λ_{ans} and λ_{prior} are weighting hyperparameters. During inference, given the input x , LLM samples latent thoughts via Eq. (3) and decodes the answer. By default, LTF uses a single trajectory for efficiency. With larger test-time budgets, it can adaptively sample multiple latent trajectories via tree of latent thoughts [14] without decoding long explicit reasoning chains.

Table 1: Performance comparison under finetuning setting across different backbones. We report the averaged Accuracy (Acc. %) and Reasoning Length (# L).

Model	Method	GSM8K-Aug		ASDiv-Aug		DU		Average	
		Acc.(↑)	# L(↓)	Acc.(↑)	# L(↓)	Acc.(↑)	# L(↓)	Acc.(↑)	# L(↓)
LLaMA-3.2 Instruct 1B	CoT	15.70	120.37	40.85	120.73	33.18	120.01	29.91	120.37
	Assist-CoT	16.30	119.85	42.18	119.53	35.34	119.58	31.27	119.65
	SoftCoT++	17.04	119.73	45.72	119.48	38.18	119.70	33.65	119.64
	iCoT	19.80	0.00	46.36	0.00	41.37	0.00	35.84	0.00
	CODI	13.30	6.00	43.93	6.00	38.06	6.00	31.76	6.00
	Coconut	20.50	6.00	53.18	6.00	43.97	6.00	39.22	6.00
	CoLaR	26.60	5.63	67.19	5.19	50.12	4.17	47.97	5.00
	ReGuLaR	34.58	3.69	72.19	1.24	59.92	1.20	55.56	2.04
	LTF	37.09	3.34	75.11	1.22	66.83	1.18	59.68	1.91
LLaMA-3.2 Instruct 3B	CoT	17.10	121.39	51.08	121.67	48.90	121.75	39.03	121.60
	Assist-CoT	17.90	120.98	52.42	120.11	50.28	120.04	40.20	120.38
	SoftCoT++	18.59	120.77	56.39	119.97	53.31	119.85	42.76	120.20
	iCoT	21.57	0.00	58.45	0.00	54.18	0.00	44.73	0.00
	Coconut	32.71	6.00	66.76	6.00	57.23	6.00	52.23	6.00
	CoLaR	42.58	5.48	73.05	5.17	61.29	4.15	58.97	4.93
	ReGuLaR	45.59	3.89	79.46	1.24	70.31	1.18	65.12	2.10
	LTF	48.30	3.42	84.04	1.21	76.82	1.17	68.85	1.95
	LLaMA-3.1 Instruct 8B	CoT	19.17	121.30	89.23	121.93	65.67	121.04	58.02
Assist-CoT		19.93	121.04	89.48	121.51	65.82	120.39	58.41	120.98
SoftCoT++		20.86	120.76	90.09	120.52	68.89	120.15	59.95	120.48
iCoT		24.24	0.00	91.03	0.00	71.27	0.00	62.18	0.00
Coconut		36.10	6.00	91.09	6.00	73.74	6.00	66.98	6.00
CoLaR		45.19	5.62	91.12	5.51	76.59	4.18	70.97	5.10
ReGuLaR		50.14	3.93	92.00	1.28	81.06	1.19	74.40	2.13
LTF		53.14	3.37	94.02	1.24	84.09	1.20	77.08	1.94
DeepSeek-R1 Distill-Qwen 1.5B		CoT	15.94	121.57	45.70	120.70	37.02	120.09	32.89
	Assist-CoT	17.36	120.81	46.48	119.81	38.62	119.67	34.15	120.10
	SoftCoT++	18.19	120.64	48.51	119.93	43.04	119.83	36.58	120.13
	iCoT	18.87	0.00	48.53	0.00	43.18	0.00	36.86	0.00
	Coconut	24.91	6.00	56.85	6.00	46.46	6.00	42.74	6.00
	CoLaR	27.38	5.71	69.36	5.23	50.35	4.17	49.03	5.04
	ReGuLaR	34.69	3.54	75.59	1.21	63.91	1.19	58.06	1.98
	LTF	36.94	3.27	79.75	1.20	69.80	1.17	62.16	1.88

4 Experiments

Tasks, Metrics & Baselines. We evaluate LTF on multiple LLM backbones, including LLaMA-3.2 1B/3B [3], LLaMA-3.1 8B [3], and DeepSeek-R1-Distill-Qwen-1.5B [50]. Following priors, we train and evaluate on GSM8K-Aug [51], ASDiv-Aug [20], and DU [52], covering math reasoning, word problems, and data understanding. To test generalization and difficulty scalability, we further evaluate on out-of-domain math datasets, including GSM-Hard [6], SVAMP [53], MultiArith [54], AQUA-RAT [55], and MATH [56]. We report two standard metrics [18, 41, 42]: Accuracy (Acc.), measuring the percentage of correct answers, and Reasoning Length (# L), measuring the number of reasoning steps per question. All results are averaged over five independent runs with different random seeds. We compare LTF with explicit reasoning methods, including CoT [11] and Assist-CoT [20], as well as latent reasoning methods, including iCoT [16], CODI [19], Coconut [18], SoftCoT++ [21], CoLaR [41], and ReGuLaR [42]. All baselines follow their default configurations for fair comparison.

We train LTF with LoRA using rank $r = 128$ and scaling factor $\alpha = 32$, and AdamW [57] with learning rate 1×10^{-4} , weight decay 1×10^{-2} , global batch size 256, and 100 training epochs on RTX PRO 6000 GPUs. For fairness, all methods use the same training budget and stop once either the epoch limit or time budget is reached. We select the checkpoint with the best validation accuracy. During inference, generation uses temperature 0.9 and top- p 0.95. See more details in Appendix B.

4.1 Main Results

Results of Finetuning. Table 1 compares LTF with explicit and latent reasoning baselines on three mathematical reasoning datasets. LTF achieves the best accuracy–efficiency tradeoffs across tasks. Compared with the strongest baseline ReGuLaR, LTF (LLaMA-1B) improves the average accuracy from 34.58% to 37.09%, while reducing the average reasoning length from 3.69 to 3.34 on the challenging GSM8K-Aug task. This suggests that LTF is effective for problems requiring stronger multi-step arithmetic reasoning, where compact latent transitions can preserve task-relevant

Table 2: Extreme compression performance of LTF under finetuning setting. We report the averaged Accuracy (Acc. %) and Reasoning Length (# L).

Dataset	Method	LLaMA-1B		LLaMA-3B		LLaMA-8B		DS-1.5B		Average	
		Acc.(↑)	# L(↓)	Acc.(↑)	# L(↓)	Acc.(↑)	# L(↓)	Acc.(↑)	# L(↓)	Acc.(↑)	# L(↓)
MATH	Coconut	5.18	6.00	7.72	6.00	8.68	6.00	6.67	6.00	7.06	6.00
	CoLaR	5.31	58.29	8.35	60.44	9.13	67.19	11.13	62.20	8.48	62.03
	ReGuLaR	6.62	1.00	11.80	1.00	13.90	1.00	15.60	1.00	11.98	1.00
	LTF	8.10	1.00	16.18	1.00	17.31	1.00	17.20	1.00	14.70	1.00
AQUA-RAT	Coconut	23.17	6.00	26.31	6.00	30.94	6.00	27.81	6.00	27.06	6.00
	CoLaR	23.69	18.60	32.78	28.20	34.52	20.30	34.33	27.00	31.33	23.53
	ReGuLaR	37.28	1.00	39.12	1.00	42.41	1.00	39.07	1.00	39.47	1.00
	LTF	39.43	1.00	43.18	1.00	46.62	1.00	43.07	1.00	43.08	1.00

Table 3: Performance comparison under transfer learning setting across different backbones. We report the averaged Accuracy (Acc. %) and Reasoning Length (# L).

Model	Method	GSM-Hard		SVAMP		MultiArith		Average	
		Acc.(↑)	# L(↓)	Acc.(↑)	# L(↓)	Acc.(↑)	# L(↓)	Acc.(↑)	# L(↓)
LLaMA-3.2 Instruct 1B	CoT	2.74	120.46	27.17	120.80	28.29	120.14	19.40	120.47
	Assist-CoT	3.02	125.19	28.04	123.02	30.06	121.86	20.37	123.36
	SoftCoT++	3.77	123.56	30.96	123.42	32.13	120.66	22.29	122.55
	iCoT	3.82	0.00	36.42	0.00	38.19	0.00	26.14	0.00
	CODI	2.94	6.00	21.65	6.00	19.20	6.00	14.60	6.00
	Coconut	4.87	6.00	38.90	6.00	41.30	6.00	28.36	6.00
	CoLaR	6.22	7.03	47.22	2.94	86.93	3.22	46.79	4.40
	ReGuLaR	8.25	4.10	48.19	2.10	88.97	2.29	48.47	2.83
	LTF	8.71	3.97	52.01	2.11	90.37	2.17	50.36	2.75
LLaMA-3.2 Instruct 3B	CoT	3.84	121.68	34.01	121.52	35.16	121.54	24.34	121.58
	Assist-CoT	4.16	125.03	35.06	123.42	37.03	121.98	25.42	123.48
	SoftCoT++	5.21	124.72	38.89	122.96	40.26	121.74	28.12	123.14
	iCoT	5.19	0.00	44.98	0.00	46.42	0.00	32.19	0.00
	Coconut	7.34	6.00	52.47	6.00	58.79	6.00	39.53	6.00
	CoLaR	9.73	6.46	60.70	2.72	90.10	3.04	53.51	4.07
	ReGuLaR	11.20	3.73	62.32	2.23	91.27	2.17	54.93	2.71
	LTF	11.88	3.64	65.48	2.14	92.94	2.10	56.77	2.63
	LLaMA-3.1 Instruct 8B	CoT	4.51	121.66	37.43	121.56	38.82	121.84	26.92
Assist-CoT		4.75	125.59	38.62	124.62	40.60	122.64	27.99	124.28
SoftCoT++		5.91	124.82	42.85	123.82	43.19	121.98	30.65	123.54
iCoT		5.82	0.00	49.48	0.00	50.39	0.00	35.23	0.00
Coconut		8.26	6.00	57.18	6.00	62.41	6.00	42.62	6.00
CoLaR		10.97	6.53	61.30	2.83	93.80	3.14	55.36	4.17
ReGuLaR		12.53	3.92	68.54	2.07	95.28	2.26	58.78	2.75
LTF		13.19	3.70	72.29	2.09	97.18	2.16	60.89	2.65
DeepSeek-R1 Distill-Qwen 1.5B		CoT	2.81	120.78	27.23	121.48	28.33	121.53	19.46
	Assist-CoT	3.07	126.03	28.12	123.76	30.14	122.70	20.44	124.16
	SoftCoT++	3.86	123.72	31.02	123.26	32.18	121.92	22.35	122.97
	iCoT	3.83	0.00	36.49	0.00	38.24	0.00	26.19	0.00
	Coconut	4.96	6.00	38.98	6.00	41.31	6.00	28.41	6.00
	CoLaR	6.32	7.03	47.27	2.94	87.01	3.22	46.86	4.40
	ReGuLaR	8.33	4.10	48.20	2.10	89.04	2.29	48.52	2.83
	LTF	8.83	3.94	52.76	2.08	91.10	2.21	50.90	2.74

information. In addition, LTF (LLaMA-8B) improves the average accuracy from 50.14% to 53.14%, while reducing the average reasoning length from 3.93 to 3.37, showing the robust scalability across backbones. On the other tasks, LTF adaptively allocates reasoning budgets for accuracy gains. On ASDiv-Aug, LTF improves the average accuracy from 92.00% to 94.02%, reducing reasoning length from 1.28 to 1.24. We attribute the performance to the entropy-weighted SubTB objective, which encourages compact and informative latent thought states rather than redundant reasoning trajectories.

Extreme Compression Evaluation. Although accuracy decreases under extreme compression, Table 2 shows that LTF consistently outperforms baselines across all settings on both LLM backbones, verifying its advantage in preserving semantic information. Compared with ReGuLaR, LTF improves the average accuracy by 2.72% on MATH and 3.61% on AQUA-RAT, demonstrating its superior ability to preserve task-relevant semantic information under compression.

Results of Transfer Learning. Table 3 compares LTF with baseline methods on transfer learning tasks across three datasets and four backbones. LTF achieves the highest average accuracy for all

Table 4: Ablation on entropy weighting and training rollout sample size S in LTF using the LLaMA-3.1 Instruct 1B backbone. We report the averaged Accuracy (Acc. %) and Reasoning Length (# L).

Settings		GSM8K-Aug		ASDiv-Aug		DU		Average	
Entropy Weighting	S	Acc.(\uparrow)	# L(\downarrow)	Acc.(\uparrow)	# L(\downarrow)	Acc.(\uparrow)	# L(\downarrow)	Acc.(\uparrow)	# L(\downarrow)
-	5	34.78	3.31	72.74	1.20	63.50	1.19	57.01	1.90
✓	5	35.19	3.33	73.42	1.23	63.61	1.19	57.41	1.92
-	10	36.10	3.30	74.08	1.19	65.02	1.19	58.40	1.89
✓	10	36.71	3.33	74.65	1.21	65.84	1.18	59.07	1.91
-	20	36.64	3.31	74.80	1.20	64.74	1.19	58.73	1.90
✓	20	37.09	3.34	75.11	1.22	66.83	1.18	59.68	1.91

Table 5: Ablation on latent thought exploration objective using the LLaMA-3.1 Instruct 1B backbone. We report the averaged Accuracy (Acc. %) and Reasoning Length (# L).

Model	GSM8K-Aug		ASDiv-Aug		DU		Average	
	Acc.(\uparrow)	# L(\downarrow)	Acc.(\uparrow)	# L(\downarrow)	Acc.(\uparrow)	# L(\downarrow)	Acc.(\uparrow)	# L(\downarrow)
GRPO	25.93	13.17	66.93	12.45	49.62	11.14	47.49	12.25
DB	35.17	7.73	72.28	7.19	60.48	6.92	55.98	7.28
TB	35.84	8.01	73.05	7.39	61.52	7.14	56.80	7.51
LTF	37.09	3.34	75.11	1.22	66.83	1.18	59.68	1.91

backbones, improving over ReGuLaR by 1.89%, 1.84%, 2.11%, and 2.38% on LLaMA-1B, LLaMA-3B, LLaMA-8B, and DS-1.5B, respectively. Meanwhile, LTF maintains a more concise reasoning length than ReGuLaR and explicit CoT in all settings. These results validate the reasoning generalization ability of LTF, improving broader reasoning performance while preserving strong compression efficiency. Additional results with 95% confidence interval are provided in Appendix C.1.

4.2 Ablation Studies

We conduct ablation studies on the key components of LTF. Due to the space limitation, we defer the analyses of reference-prior regularization and test-time scaling to Appendix C.1.

Analysis on Hyperparameters. Table 4 studies entropy weighting and rollout sample size S in LTF. **1)** Entropy weighting consistently improves accuracy with little change in reasoning length, and its gains increase with larger S (+0.40%, +0.67%, and +0.95% for $S = 5, 10, 20$), suggesting stronger benefits when sampled subtrajectories are more diverse. It enables effective credit assignment to improve reasoning performance over uniform SubTB. **2)** Increasing S improves performance by expanding trajectory diversity: with entropy weighting, average accuracy rises from 57.41% to 59.68% as S increases from 5 to 20, showing the scaling effect during training.

Analysis on Latent Thought Exploration Objective. Table 5 studies the latent thought exploration objective in LTF. Baseline details are provided in Appendix B.1. **1)** Compared with GRPO, GFlowNet-based objectives achieve substantially better accuracy–length tradeoffs. DB improves the average accuracy from 47.49% to 55.98% while reducing the average reasoning length from 12.25 to 7.28, suggesting that flow-based learning provides more structured supervision for latent thought exploration than standard RL. **2)** LTF achieves the best overall tradeoff. It obtains the highest average accuracy of 59.68% while reducing the average reasoning length to only 1.91. These results show that LTF better aligns latent thought exploration with both reasoning effectiveness and conciseness.

5 Conclusion

We introduce LTF, a framework for efficient latent reasoning in LLMs. LTF models reasoning as variable-length continuous latent trajectories and trains the sampler with a continuous GFlowNet objective, allocating probability mass according to answer quality and computational cost. An entropy-weighted subtrajectory balance objective and a reference-prior regularizer further improve exploration and stability. Extensive experiments highlight the superiority of LTF over explicit and latent reasoning methods, showing a path towards a better reasoning accuracy–efficiency frontier.

Limitations. Our experiments primarily focus on textual tasks involving words and symbols; extending to other modalities, such as vision and speech, remains as future work. In addition, we will further explore the generalization ability of Latent Thought Flow in theory.

References

- [1] Josh Achiam, Steven Adler, Sandhini Agarwal, Lama Ahmad, Ilge Akkaya, Florencia Leoni Aleman, Diogo Almeida, Janko Altenschmidt, Sam Altman, Shyamal Anadkat, et al. Gpt-4 technical report. *arXiv preprint arXiv:2303.08774*, 2023. **1**
- [2] Aaditya Singh, Adam Fry, Adam Perelman, Adam Tart, Adi Ganesh, Ahmed El-Kishky, Aidan McLaughlin, Aiden Low, AJ Ostrow, Akhila Ananthram, et al. Openai gpt-5 system card. *arXiv preprint arXiv:2601.03267*, 2025.
- [3] Aaron Grattafiori, Abhimanyu Dubey, Abhinav Jauhri, Abhinav Pandey, Abhishek Kadian, Ahmad Al-Dahle, Aiesha Letman, Akhil Mathur, Alan Schelten, Alex Vaughan, et al. The llama 3 herd of models. *arXiv preprint arXiv:2407.21783*, 2024. **7**
- [4] Gemini Team, Rohan Anil, Sebastian Borgeaud, Jean-Baptiste Alayrac, Jiahui Yu, Radu Soricut, Johan Schalkwyk, Andrew M Dai, Anja Hauth, Katie Millican, et al. Gemini: a family of highly capable multimodal models. *arXiv preprint arXiv:2312.11805*, 2023. **1**
- [5] Hunter Lightman, Vineet Kosaraju, Yuri Burda, Harrison Edwards, Bowen Baker, Teddy Lee, Jan Leike, John Schulman, Ilya Sutskever, and Karl Cobbe. Let’s verify step by step. In *The twelfth international conference on learning representations*, 2023. **1**
- [6] Luyu Gao, Aman Madaan, Shuyan Zhou, Uri Alon, Pengfei Liu, Yiming Yang, Jamie Callan, and Graham Neubig. Pal: Program-aided language models. In *International conference on machine learning*, pages 10764–10799. PMLR, 2023. **1, 7**
- [7] Noah Shinn, Federico Cassano, Ashwin Gopinath, Karthik Narasimhan, and Shunyu Yao. Reflexion: Language agents with verbal reinforcement learning. *Advances in neural information processing systems*, 36:8634–8652, 2023. **1**
- [8] Shibo Hao, Yi Gu, Haodi Ma, Joshua Hong, Zhen Wang, Daisy Wang, and Zhiting Hu. Reasoning with language model is planning with world model. In *Proceedings of the 2023 Conference on Empirical Methods in Natural Language Processing*, pages 8154–8173, 2023. **1**
- [9] Yujia Li, David Choi, Junyoung Chung, Nate Kushman, Julian Schrittwieser, Rémi Leblond, Tom Eccles, James Keeling, Felix Gimeno, Agustin Dal Lago, et al. Competition-level code generation with alphacode. *Science*, 378(6624):1092–1097, 2022. **1**
- [10] Erik Nijkamp, Bo Pang, Hiroaki Hayashi, Lifu Tu, Huan Wang, Yingbo Zhou, Silvio Savarese, and Caiming Xiong. Codegen: An open large language model for code with multi-turn program synthesis. *arXiv preprint arXiv:2203.13474*, 2022. **1**
- [11] Jason Wei, Xuezhi Wang, Dale Schuurmans, Maarten Bosma, Fei Xia, Ed Chi, Quoc V Le, Denny Zhou, et al. Chain-of-thought prompting elicits reasoning in large language models. *Advances in neural information processing systems*, 35:24824–24837, 2022. **1, 2, 7, 14**
- [12] Takeshi Kojima, Shixiang Shane Gu, Machel Reid, Yutaka Matsuo, and Yusuke Iwasawa. Large language models are zero-shot reasoners. *Advances in neural information processing systems*, 35:22199–22213, 2022. **1, 2**
- [13] Xuezhi Wang, Jason Wei, Dale Schuurmans, Quoc Le, Ed Chi, Sharan Narang, Aakanksha Chowdhery, and Denny Zhou. Self-consistency improves chain of thought reasoning in language models. *arXiv preprint arXiv:2203.11171*, 2022. **1, 2**
- [14] Shunyu Yao, Dian Yu, Jeffrey Zhao, Izhak Shafran, Tom Griffiths, Yuan Cao, and Karthik Narasimhan. Tree of thoughts: Deliberate problem solving with large language models. *Advances in neural information processing systems*, 36:11809–11822, 2023. **1, 2, 6**
- [15] Sachin Goyal, Ziwei Ji, Ankit Singh Rawat, Aditya Krishna Menon, Sanjiv Kumar, and Vaishnavh Nagarajan. Think before you speak: Training language models with pause tokens. *arXiv preprint arXiv:2310.02226*, 2023. **1, 2**
- [16] Yuntian Deng, Yejin Choi, and Stuart Shieber. From explicit cot to implicit cot: Learning to internalize cot step by step. *arXiv preprint arXiv:2405.14838*, 2024. **1, 2, 7, 14**

- [17] Jeffrey Cheng and Benjamin Van Durme. Compressed chain of thought: Efficient reasoning through dense representations. *arXiv preprint arXiv:2412.13171*, 2024. 1, 2
- [18] Shibo Hao, Sainbayar Sukhbaatar, DiJia Su, Xian Li, Zhiting Hu, Jason Weston, and Yuandong Tian. Training large language models to reason in a continuous latent space. *arXiv preprint arXiv:2412.06769*, 2024. 1, 7, 14
- [19] Zhenyi Shen, Hanqi Yan, Linhai Zhang, Zhanghao Hu, Yali Du, and Yulan He. Codi: Compressing chain-of-thought into continuous space via self-distillation. In *Proceedings of the 2025 Conference on Empirical Methods in Natural Language Processing*, pages 677–693, 2025. 7, 14
- [20] Yige Xu, Xu Guo, Zhiwei Zeng, and Chunyan Miao. Softcot: Soft chain-of-thought for efficient reasoning with llms. In *Proceedings of the 63rd Annual Meeting of the Association for Computational Linguistics (Volume 1: Long Papers)*, pages 23336–23351, 2025. 7, 14
- [21] Yige Xu, Xu Guo, Zhiwei Zeng, and Chunyan Miao. Softcot++: Test-time scaling with soft chain-of-thought reasoning. *arXiv preprint arXiv:2505.11484*, 2025. 2, 7, 14
- [22] Cong Jiang, Xiaofeng Zhang, Fangzhi Zhu, XiaoWei Chen, Junxiong Zhu, and Zheng Zhang. Rethinking llm reasoning: From explicit trajectories to latent representations. In *The Fourteenth International Conference on Learning Representations*, 2026. 2
- [23] Zhenrui Yue, Bowen Jin, Huimin Zeng, Honglei Zhuang, Zhen Qin, Jinsung Yoon, Lanyu Shang, Jiawei Han, and Dong Wang. Hybrid latent reasoning via reinforcement learning. *arXiv preprint arXiv:2505.18454*, 2025. 3
- [24] Yiran Zhao, Yuhui Xu, Doyen Sahoo, Caiming Xiong, and Junnan Li. Learning to reason over continuous tokens with reinforcement learning. In *The Fourteenth International Conference on Learning Representations*, 2026. 1, 3
- [25] Emmanuel Bengio, Moksh Jain, Maksym Korablyov, Doina Precup, and Yoshua Bengio. Flow network based generative models for non-iterative diverse candidate generation. *Advances in neural information processing systems*, 34:27381–27394, 2021. 2, 3, 5, 15
- [26] Yoshua Bengio, Salem Lahlou, Tristan Deleu, Edward J Hu, Mo Tiwari, and Emmanuel Bengio. Gflownet foundations. *Journal of Machine Learning Research*, 24(210):1–55, 2023. 2, 3, 5
- [27] Edward J Hu, Moksh Jain, Eric Elmoznino, Younesse Kaddar, Guillaume Lajoie, Yoshua Bengio, and Nikolay Malkin. Amortizing intractable inference in large language models. *arXiv preprint arXiv:2310.04363*, 2023. 2, 3
- [28] Ryoichi Takase, Masaya Tsunokake, Yuta Tsuchiya, and Shota Inuzuka. Gflownet fine-tuning for diverse correct solutions in mathematical reasoning tasks. *arXiv preprint arXiv:2410.20147*, 2024.
- [29] Haoqiang Kang, Enna Sachdeva, Piyush Gupta, Sangjae Bae, and Kwonjoon Lee. Gflowvlm: Enhancing multi-step reasoning in vision-language models with generative flow networks. In *Proceedings of the Computer Vision and Pattern Recognition Conference*, pages 3815–3825, 2025. 2, 3
- [30] Salem Lahlou, Tristan Deleu, Pablo Lemos, Dinghuai Zhang, Alexandra Volokhova, Alex Hernández-García, Léna Néhale Ezzine, Yoshua Bengio, and Nikolay Malkin. A theory of continuous generative flow networks. In *International Conference on Machine Learning*, pages 18269–18300. PMLR, 2023. 2, 3
- [31] Nikolay Malkin, Moksh Jain, Emmanuel Bengio, Chen Sun, and Yoshua Bengio. Trajectory balance: Improved credit assignment in gflownets. *Advances in Neural Information Processing Systems*, 35:5955–5967, 2022. 2, 3, 15
- [32] Kanika Madan, Jarrid Rector-Brooks, Maksym Korablyov, Emmanuel Bengio, Moksh Jain, Andrei Cristian Nica, Tom Bosc, Yoshua Bengio, and Nikolay Malkin. Learning gflownets from partial episodes for improved convergence and stability. In *International Conference on Machine Learning*, pages 23467–23483. PMLR, 2023. 2, 5

- [33] Pan Lu, Swaroop Mishra, Tanglin Xia, Liang Qiu, Kai-Wei Chang, Song-Chun Zhu, Oyvind Tafjord, Peter Clark, and Ashwin Kalyan. Learn to explain: Multimodal reasoning via thought chains for science question answering. *Advances in neural information processing systems*, 35: 2507–2521, 2022. 2
- [34] Zhuosheng Zhang, Aston Zhang, Mu Li, Hai Zhao, George Karypis, and Alex Smola. Multi-modal chain-of-thought reasoning in language models. *arXiv preprint arXiv:2302.00923*, 2023. 2, 6
- [35] Hao Shao, Shengju Qian, Han Xiao, Guanglu Song, Zhuofan Zong, Letian Wang, Yu Liu, and Hongsheng Li. Visual cot: Advancing multi-modal language models with a comprehensive dataset and benchmark for chain-of-thought reasoning. *Advances in Neural Information Processing Systems*, 37:8612–8642, 2024. 2, 6
- [36] Zhengyuan Yang, Linjie Li, Jianfeng Wang, Kevin Lin, Ehsan Azarnasab, Faisal Ahmed, Zicheng Liu, Ce Liu, Michael Zeng, and Lijuan Wang. Mm-react: Prompting chatgpt for multimodal reasoning and action. *arXiv preprint arXiv:2303.11381*, 2023. 2
- [37] Dídac Surís, Sachit Menon, and Carl Vondrick. Vipergpt: Visual inference via python execution for reasoning. In *Proceedings of the IEEE/CVF international conference on computer vision*, pages 11888–11898, 2023. 2
- [38] Lihao Sun, Hang Dong, Bo Qiao, Qingwei Lin, Dongmei Zhang, and Saravan Rajmohan. Llm reasoning as trajectories: Step-specific representation geometry and correctness signals. *arXiv preprint arXiv:2604.05655*, 2026. 2
- [39] Keshav Ramji, Tahira Naseem, and Ramón Fernandez Astudillo. Learning efficient latent reasoning with abstract chain-of-thought. In *Workshop on Latent {&} Implicit Thinking {&} Going Beyond CoT Reasoning*, 2026. 2
- [40] Deqian Kong, Minglu Zhao, Dehong Xu, Bo Pang, Shu Wang, Edouardo Honig, Zhangzhang Si, Chuan Li, Jianwen Xie, Sirui Xie, et al. Latent thought models with variational bayes inference-time computation. *arXiv preprint arXiv:2502.01567*, 2025. 2
- [41] Wenhui Tan, Jiaze Li, Jianzhong Ju, Zhenbo Luo, Ruihua Song, and Jian Luan. Think silently, think fast: Dynamic latent compression of llm reasoning chains. *arXiv preprint arXiv:2505.16552*, 2025. 4, 7, 15
- [42] Fanmeng Wang, Haotian Liu, Guojiang Zhao, Hongteng Xu, and Zhifeng Gao. Regular: Variational latent reasoning guided by rendered chain-of-thought. *arXiv preprint arXiv:2601.23184*, 2026. 2, 4, 7, 15
- [43] Hanwen Du, Yuxin Dong, and Xia Ning. Latent thinking optimization: Your latent reasoning language model secretly encodes reward signals in its latent thoughts. *arXiv preprint arXiv:2509.26314*, 2025. 3, 5
- [44] Yuyan Zhou, Jiarui Yu, Hande Dong, Zhezhen Hao, Hong Wang, Jianqing Zhang, and Qiang Lin. Lepo: Latent reasoning policy optimization for large language models. *arXiv e-prints*, pages arXiv–2604, 2026. 3
- [45] Fangxu Yu, Lai Jiang, Haoqiang Kang, Shibo Hao, and Lianhui Qin. Flow of reasoning: Training llms for divergent reasoning with minimal examples. *arXiv preprint arXiv:2406.05673*, 2024. 3
- [46] Xuekai Zhu, Daixuan Cheng, Dinghuai Zhang, Hengli Li, Kaiyan Zhang, Che Jiang, Youbang Sun, Ermo Hua, Yuxin Zuo, Xingtai Lv, et al. Flowrl: Matching reward distributions for llm reasoning. *arXiv preprint arXiv:2509.15207*, 2025. 3, 5
- [47] Guohao Sun, Hang Hua, Jian Wang, Jiebo Luo, Sohail Dianat, Majid Rabbani, Raghuveer Rao, and Zhiqiang Tao. Latent chain-of-thought for visual reasoning. *arXiv preprint arXiv:2510.23925*, 2025. 3
- [48] Diederik P Kingma and Max Welling. Auto-encoding variational bayes. *arXiv preprint arXiv:1312.6114*, 2013. 4

- [49] Tiago Silva, Rodrigo Barreto Alves, Eliezer de Souza da Silva, Amauri H Souza, Vikas Garg, Samuel Kaski, and Diego Mesquita. When do gflownets learn the right distribution? In *The Thirteenth International Conference on Learning Representations*, 2025. 5
- [50] Daya Guo, Dejian Yang, Haowei Zhang, Junxiao Song, Peiyi Wang, Qihao Zhu, Runxin Xu, Ruoyu Zhang, Shirong Ma, Xiao Bi, et al. Deepseek-r1: Incentivizing reasoning capability in llms via reinforcement learning. *arXiv preprint arXiv:2501.12948*, 2025. 7
- [51] Yuntian Deng, Kiran Prasad, Roland Fernandez, Paul Smolensky, Vishrav Chaudhary, and Stuart Shieber. Implicit chain of thought reasoning via knowledge distillation. *arXiv preprint arXiv:2311.01460*, 2023. 7
- [52] Aarohi Srivastava, Abhinav Rastogi, Abhishek Rao, Abu Awal Md Shoeb, Abubakar Abid, Adam Fisch, Adam R Brown, Adam Santoro, Aditya Gupta, Adrià Garriga-Alonso, et al. Beyond the imitation game: Quantifying and extrapolating the capabilities of language models. *Transactions on machine learning research*, 2023. 7
- [53] Arkil Patel, Satwik Bhattamishra, and Navin Goyal. Are nlp models really able to solve simple math word problems? In *Proceedings of the 2021 conference of the North American chapter of the association for computational linguistics: human language technologies*, pages 2080–2094, 2021. 7
- [54] Subhro Roy and Dan Roth. Solving general arithmetic word problems. In *Proceedings of the 2015 conference on empirical methods in natural language processing*, pages 1743–1752, 2015. 7
- [55] Wang Ling, Dani Yogatama, Chris Dyer, and Phil Blunsom. Program induction by rationale generation: Learning to solve and explain algebraic word problems. In *Proceedings of the 55th annual meeting of the association for computational linguistics (volume 1: Long papers)*, pages 158–167, 2017. 7
- [56] Dan Hendrycks, Collin Burns, Saurav Kadavath, Akul Arora, Steven Basart, Eric Tang, Dawn Song, and Jacob Steinhardt. Measuring mathematical problem solving with the math dataset. *arXiv preprint arXiv:2103.03874*, 2021. 7
- [57] Ilya Loshchilov and Frank Hutter. Decoupled weight decay regularization. *arXiv preprint arXiv:1711.05101*, 2017. 7
- [58] Zhihong Shao, Peiyi Wang, Qihao Zhu, Runxin Xu, Junxiao Song, Xiao Bi, Haowei Zhang, Mingchuan Zhang, YK Li, Yang Wu, et al. Deepseekmath: Pushing the limits of mathematical reasoning in open language models. *arXiv preprint arXiv:2402.03300*, 2024. 15

A Notation Definitions

The major notations used in this paper are listed in Table 6.

Table 6: Major Notations.

Notation	Definition
x	Input question.
y	Target answer.
h_x	Embedding of the input x produced by the backbone encoder, i.e., $h_x = p_\phi(x)$.
\mathbf{z}_t	Continuous latent thought sampled at step t .
s_t	Context state $(h_x, z_{1:t})$.
T	Number of latent thoughts in τ
\perp	Stop token indicating termination of the latent trajectory.
$\tau = (\mathbf{z}_{1:T}, \perp)$	Variable-length latent thought trajectory ending with stop token \perp .
$q_\varphi(\mathbf{z}_{t+1} s_t)$	Continuous latent thought transition density.
$p_\psi(\langle \text{eos}_r \rangle s_t)$	Stopping probability of latent reasoning at prefix state s_t .
$\pi^\perp(s_t)$	Shorthand for $p_\psi(\langle \text{eos}_r \rangle s_t)$.
$F(s_t)$	Flow assigned to state s_t .
$\mathcal{R}_{x,y}(s_t \rightarrow \perp)$	Terminal reward for stopping from state s_t given the input x and target y .
$\chi_{i:j}$	Continuous SubTB residual over subtrajectories $s_i \rightarrow \dots \rightarrow s_j$.

B Additional Implementation Details

In this section, we provide comprehensive details regarding baselines and training details.

B.1 Baseline Details

For the main experiments, we employ various explicit and latent-based reasoning methods as baselines. The reported metric reasoning length ($\#L$) measures the number of reasoning steps before producing the final answer: for explicit reasoning methods, this corresponds to the number of explicit reasoning tokens; for latent reasoning approaches, it corresponds to the number of latent reasoning steps; and for implicit one-pass methods such as iCoT, $\#L$ is defined as 0. Importantly, latent reasoning methods typically implement each latent step with approximately the same forward computation as one explicit decoding step, resulting in comparable per-step computational overhead in different reasoning paradigms. Thus, $\#L$ serves as a practical metric for evaluating reasoning efficiency across both explicit and latent reasoning frameworks. The detailed description of the above baselines is provided below:

CoT [11]: This baseline uses chain-of-thought prompting templates to elicit explicit intermediate reasoning steps before producing the final answer.

Assist-CoT [20]: This baseline uses a smaller assistant model to generate explicit reasoning tokens, which are then provided to the LLM as chain-of-thought prompts. The reasoning length ($\#L$) includes both soft thought tokens and intermediate reasoning steps.

SoftCoT++ [21]: This method generates multiple diverse soft thought representations through specialized initial tokens, and further encourages diversity among them with a contrastive learning objective. These soft thoughts are then used to guide the LLM’s explicit reasoning process. The reasoning length ($\#L$) includes both soft thought tokens and intermediate reasoning steps.

iCoT [16]: This baseline progressively drops intermediate reasoning steps during fine-tuning, encouraging the model to internalize the reasoning process while preserving task performance.

CODI [19]: This baseline uses self-distillation to align the hidden activations of latent thoughts with CoT trajectories, thereby transferring explicit reasoning patterns into the latent space.

Coconut [18]: This baseline recursively feeds the last hidden state of the LLM back as a latent thought embedding, using it as the next-step input to support subsequent reasoning.

CoLaR [41]: This baseline dynamically compresses reasoning chains into latent variables, where each latent state summarizes multiple consecutive reasoning tokens. It trains a latent head to autoregressively predict compressed embeddings and uses reinforcement learning to encourage diverse and concise latent reasoning paths.

ReGuLaR [42]: This baseline formulates latent reasoning within a variational framework, where latent reasoning states are sampled from posterior distributions conditioned on previous states. It renders explicit CoT segments as images and uses their visual representations to regularize the latent states.

For ablation studies, we employ RL- and GFlowNet-based methods as baselines. The detailed description of the above baselines is provided below:

GRPO [58]: This baseline samples a group of outputs $\{o_1, o_2, \dots, o_G\}$ from the old policy $p_{\Theta_{\text{old}}}$, where G denotes the group size. Each output o_i consists of a latent reasoning trajectory τ_i and a final answer. GRPO then optimizes the current policy p_{Θ} by minimizing the following clipped objective:

$$\mathcal{L}_{\text{GRPO}} = -\frac{1}{G} \sum_{i=1}^G \min \left(\frac{p_{\Theta}(o_i | x)}{p_{\Theta_{\text{old}}}(o_i | x)} A_i, \text{clip} \left(\frac{p_{\Theta}(o_i | x)}{p_{\Theta_{\text{old}}}(o_i | x)}, 1 - \epsilon, 1 + \epsilon \right) A_i \right). \quad (23)$$

Here, A_i is computed as a group-normalized reward:

$$A_i = \frac{r_i - \text{mean}(r_1, r_2, \dots, r_G)}{\text{std}(r_1, r_2, \dots, r_G)}. \quad (24)$$

We use $\mathcal{R}_{x,y}(\tau_i)$ as the reward, i.e.,

$$r_i = \mathcal{R}_{x,y}(\tau_i). \quad (25)$$

We replace the LTF objective Eq. (22) with $\mathcal{L}_{\text{GRPO}}$ and keep other training configurations same.

Detailed Balance (DB) [25]: This variant uses the same overall objective as LTF (Eq. (22)), but replaces $\mathcal{L}_{\text{flow}}$ with a Detailed Balance loss. It can be viewed as a one-step special case of Sub-Trajectory Balance, where flow consistency is enforced only between adjacent states. Specifically,

$$\mathcal{L}_{\text{DB}} = \mathbb{E}_{\tau \sim q_{\varphi}(\cdot | s_0)} \left[\sum_{t=0}^{T-1} \chi_{t:t+1}^2 \right], \quad (26)$$

where $\chi_{t:t+1}$ is defined in Eq. (14). All other training configurations are kept unchanged.

Trajectory Balance (TB) [31]: This variant uses the same overall objective as LTF (Eq. (22)), but replaces $\mathcal{L}_{\text{flow}}$ with a Trajectory Balance loss. Unlike DB, which enforces local one-step consistency, TB enforces flow consistency only over the complete sampled trajectory. Specifically,

$$\mathcal{L}_{\text{TB}} = \mathbb{E}_{\tau \sim q_{\varphi}(\cdot | s_0)} [\chi_{0:T}^2], \quad (27)$$

where $\chi_{0:T}$ is given by Eq. (14). All other training configurations are kept unchanged.

B.2 Training Details

For all experiments, the Latent Head in LTF is implemented as a three-layer MLP, with hidden dimensions matching the hidden size of the LLM backbone. We set `rollout_n` = 20 and $T_{\text{max}} = 32$ during training, meaning that the model samples 20 reasoning trajectories with maximum latent reasoning length of 32 for each prompt. For transfer learning settings, we use the models finetuned on GSM8K-Aug to study the out-of-domain generalization performance. In the ablation study on latent-thought exploration objectives, we use the same setting, i.e., `rollout_n` = 20 and $T_{\text{max}} = 32$, for all compared methods, including GRPO, DB, and TB, to ensure a fair comparison. Following prior work [42], we construct the reference representation r as the embedding of golden explicit rationale in the training dataset. All hyperparameters in LTF were selected by grid search on the validation set and then fixed across all experiments. We set $\lambda_c = 0.03$ to control the cost penalty in the terminal reward. In validation experiments, LTF was stable for $\lambda_c \in (0.01, 0.04)$, and we therefore use the value 0.03 as the default setting. We set $\lambda_{\text{ans}} = 1.0$ for the answer-generation loss, so that the answer objective remains on the same scale as the main training objective. For the prior loss, we use a piecewise-linear annealing schedule for λ_{prior} . Specifically, λ_{prior} is initialized to 3.0 and linearly decayed to 0.1 over 100 epochs, with the value updated every five epochs. This schedule imposes a strong prior constraint at the beginning of training and gradually relaxes the constraint as training proceeds, allowing the reward-driven objective to have a larger influence in later stages. We found that LTF is generally robust to small variations around these settings.

Table 7: Performance comparison under finetuning setting (GSM8K-Aug) and transfer learning setting (GSM-Hard, SVAMP, MultiArith) using LLaMA-3.2-1B-Instruct. We report the averaged number with 95% confidence interval on Accuracy (Acc. %) and Reasoning Length (# L).

Method	GSM8K-Aug		GSM-Hard		SVAMP		MultiArith	
	Acc.(↑)	# L(↓)	Acc.(↑)	# L(↓)	Acc.(↑)	# L(↓)	Acc.(↑)	# L(↓)
CoT	15.70 \pm 0.18	120.37 \pm 0.17	2.74 \pm 0.12	120.46 \pm 0.23	27.17 \pm 0.23	120.80 \pm 0.18	28.29 \pm 0.31	120.14 \pm 0.19
Assist-CoT	16.30 \pm 0.19	119.85 \pm 0.19	3.02 \pm 0.15	125.19 \pm 0.24	28.04 \pm 0.29	123.02 \pm 0.18	30.06 \pm 0.34	121.86 \pm 0.20
SoftCoT++	17.04 \pm 0.21	119.73 \pm 0.20	3.77 \pm 0.16	123.56 \pm 0.26	30.96 \pm 0.31	123.42 \pm 0.25	32.13 \pm 0.36	120.66 \pm 0.23
iCoT	19.80 \pm 0.22	0.00 \pm 0.00	3.82 \pm 0.16	0.00 \pm 0.00	36.42 \pm 0.52	0.00 \pm 0.00	38.19 \pm 0.64	0.00 \pm 0.00
CODI	13.30 \pm 0.64	6.00 \pm 0.00	2.94 \pm 0.24	6.00 \pm 0.00	21.65 \pm 0.70	6.00 \pm 0.00	19.20 \pm 0.82	6.00 \pm 0.00
Coconut	20.50 \pm 0.74	6.00 \pm 0.00	4.87 \pm 0.31	6.00 \pm 0.00	38.90 \pm 0.71	6.00 \pm 0.00	41.30 \pm 0.67	6.00 \pm 0.00
CoLaR	26.60 \pm 0.17	5.63 \pm 0.05	6.22 \pm 0.14	7.03 \pm 0.06	47.22 \pm 0.30	2.94 \pm 0.03	86.93 \pm 0.21	3.22 \pm 0.05
ReGuLaR	34.58 \pm 0.22	3.69 \pm 0.21	8.25 \pm 0.14	4.10 \pm 0.43	48.19 \pm 0.39	2.10 \pm 0.19	88.97 \pm 0.27	2.29 \pm 0.28
LTF	37.09 \pm 0.19	3.34 \pm 0.09	8.71 \pm 0.13	3.97 \pm 0.21	52.01 \pm 0.27	2.11 \pm 0.06	90.37 \pm 0.19	2.17 \pm 0.08

Table 8: Ablation on reference-prior regularization (RPR) using the LLaMA-3.1 Instruct 1B backbone. We report the averaged Accuracy (Acc. %) and Reasoning Length (# L).

Method	GSM8K-Aug		ASDiv-Aug		DU		Average	
	Acc.(↑)	# L(↓)	Acc.(↑)	# L(↓)	Acc.(↑)	# L(↓)	Acc.(↑)	# L(↓)
LTF	37.09	3.34	75.11	1.22	66.83	1.18	59.68	1.91
w/o RPR	37.21	3.72	75.04	2.38	65.70	2.14	59.32	2.75

Table 9: Ablation on number of latent thought chains N during test time using the LLaMA-3.1 Instruct 1B backbone. We report the averaged Accuracy (Acc. %) and Reasoning Length (# L).

N	GSM8K-Aug		ASDiv-Aug		DU		Average	
	Acc.(↑)	# L(↓)	Acc.(↑)	# L(↓)	Acc.(↑)	# L(↓)	Acc.(↑)	# L(↓)
1	37.09	3.34	75.11	1.22	66.83	1.18	59.68	1.91
5	38.13	3.38	77.62	1.24	68.03	1.20	61.26	1.94
10	38.72	3.37	78.73	1.23	68.94	1.20	62.13	1.93

C Extended Experimental Results

C.1 Extended Empirical Results

Main Results with 95% Confidence Interval. Table 7 shows finetuning and transfer learning performance comparison on reasoning datasets under LLaMA-3.2-1B-Instruct with 95% confidence interval (\pm) on Accuracy (Acc. %) and Reasoning Length (# L). These results indicate that LTF achieves better accuracy–efficiency tradeoffs across tasks. This observation can be attributed to the Entropy-Weighted SubTB objective, which encourages compact and informative latent states rather than redundant reasoning trajectories, highlighting the stability and broad applicability of LTF across model families and scales.

Ablation Analysis on Reference-Prior Regularization (RPR). Table 8 ablates the effect of reference-prior regularization (RPR) (Sec. 3.4) in LTF. Compared with LTF w/o RPR, LTF improves the average accuracy from 59.32% to 59.68%, while reducing the average latent reasoning length from 2.75 to 1.91. Notably, LTF w/o RPR slightly outperforms LTF on GSM8K-Aug (37.21 vs. 37.09), highlighting the difficulty of latent-space exploration, where optimization can become trapped in local optima. However, LTF achieves better overall performance while producing more concise reasoning paths, validating the effectiveness of RPR in stabilizing exploration.

Analysis on Test-Time Scaling. Table 9 evaluates how the number of latent thought chains N affects inference performance. Increasing N consistently improves accuracy across all three benchmarks, while leaving the average reasoning length nearly unchanged. Notably, raising N from 1 to 10 improves average accuracy from 59.68% to 62.13% (+2.45), whereas the average reasoning length changes only marginally from 1.91 to 1.93. These results demonstrate a key advantage of LTF: it supports effective test-time scaling by sampling multiple compact latent reasoning trajectories, rather

Table 10: Average reasoning entropy with 95% confidence interval of latent reasoning trajectories across different reasoning methods using the LLaMA-3.1 Instruct 8B backbone. Average reasoning entropy $\Xi(\tau)$ is calculated via Eq. (28).

Method	Average Reasoning Entropy $\Xi(\tau)$
CoLaR	0.013 ± 0.009
ReGuLaR	0.019 ± 0.002
LTF w/o EW	0.030 ± 0.006
LTF	0.024 ± 0.003

than relying on substantially longer reasoning traces. We further observe that LTF can adaptively allocate different numbers of reasoning steps to problems of varying difficulty.

This trend aligns with the intended Monte Carlo inference mechanism of LTF. By sampling more latent thought chains, the model increases the probability of identifying a high-reward reasoning trajectory. At the same time, the diminishing improvement from $N = 5$ to $N = 10$ suggests that a modest number of samples is sufficient to capture most of the attainable benefit. Overall, these results provide empirical evidence that the learned reward-induced sampling posterior distribution in LTF is effective for improving inference-time performance efficiently.

C.2 Analysis of Reasoning Trajectories

To better understand the latent reasoning dynamics learned by LTF, we analyze the average reasoning entropy of latent reasoning paths generated by CoLaR, ReGuLaR, LTF w/o entropy weighting (EW), and LTF under LLaMA-3.1 Instruct 8B backbone. Entropy quantifies how much information content the latent reasoning trajectory carries. A higher entropy often indicates a richer spread of information across many dimensions, reflecting diverse, less redundant features and better information preservation. Conversely, a lower entropy usually reflects concentrated eigenvalue spectra, suggesting that the latent representations may contain redundant information. Given a latent reasoning trajectory $\tau = (s_0, \mathbf{z}_{1:T})$, we define its *average reasoning entropy* as

$$\Xi(\tau) = \frac{1}{T} \sum_{t=0}^{T-1} \mathcal{H}[q_{\varphi}(\mathbf{z}_{t+1} | s_t)], \quad (28)$$

where $\mathcal{H}(\cdot)$ denotes differential entropy.

Our empirical study investigates the property of latent reasoning paths based on test samples drawn from fine-tuning tasks. As shown in Table 10, CoLaR exhibits the lowest reasoning entropy (0.013), suggesting that its latent reasoning trajectories are highly deterministic and potentially prone to trajectory collapse. ReGuLaR yields higher entropy (0.019), indicating that it encourages more stochastic latent reasoning behaviors. LTF w/o entropy weighting further increases the entropy (0.030), producing even more stochastic but less structured reasoning trajectories.

In contrast, LTF achieves lower entropy (0.024) than LTF w/o entropy weighting while still maintaining higher stochasticity than CoLaR and ReGuLaR. This pattern suggests that entropy-weighted sub-trajectories do not simply maximize stochasticity; rather, they regulate the degree of exploration in latent reasoning. By adaptively allocating training credit to sub-trajectories with appropriate uncertainty, LTF encourages reasoning paths that are both diverse and structured, which helps explain its stronger downstream performance.

These observations indicate the existence of an effective entropy regime for latent reasoning and we denote the threshold as *effective entropy threshold*. When reasoning entropy is too low and under the effective entropy threshold, latent trajectories may collapse into overly deterministic patterns, limiting information contained in the latent reasoning paths and weakening generalization. Moderate increases in entropy can improve reasoning performance by encouraging diverse latent trajectories. However, once entropy becomes excessive beyond the effective entropy threshold, the reasoning process may become overly stochastic, making the learned trajectories less reliable and less effective for downstream tasks. Thus, identifying the effective entropy regime is crucial for regulating latent reasoning dynamics and improving reasoning performance.

D Broader Impact

The large language models employed in this research may reflect biases or generate sensitive or potentially offensive responses, intended solely for academic and scientific purposes. The opinions expressed within generated outputs do not represent the views of the authors. We remain committed to fostering the development of AI technologies that align with ethical standards and reflect societal values.